Unsupervised sensory-motor associative learning by human brain explant in-a-dish enables movement imitation by robot

gowrishankar ganesh

gans_gs@hotmail.com

CNRS

Yukiko Iwasaki

UM-CNRS Laboratoire D'Informatique de Robotique et de Microelectronique de Montpellier (LIRMM)

Corentin bernou

CNRS - IRIM https://orcid.org/0009-0004-2309-7412

sophie colomb

Hospital CHU Montpellier

Barbara Gorda

CNRS https://orcid.org/0000-0001-5571-9942

Robin Passama

UM-CNRS Laboratoire D'Informatique de Robotique et de Microelectronique de Montpellier (LIRMM)

Raphael Gaudin

CNRS https://orcid.org/0000-0002-8558-8143

Article

Keywords:

Posted Date: June 3rd, 2026

DOI: https://doi.org/10.21203/rs.3.rs-9638576/v1

Additional Declarations: There is **NO** Competing Interest.

Unsupervised sensory-motor associative learning by human brain explant *in-a-dish* enables movement imitation by robot

Y. Iwasaki[a], C. Bernou[b], S. Coulomb[c], B. Gorda[b], R. Passama[a], R. Gaudin[b]*, G. Ganesh[a]*

[a] *UM-CNRS Laboratoire D'Informatique de Robotique et de Microelectronique de Montpellier (LIRMM), 161, Rue Ada, Montpellier, France*
[b] *CNRS, Institut de Recherche en Infectiologie de Montpellier (IRIM), 1919 Route de Mende, Montpellier, France*
[c] *Equipe de droit p´enal et sciences forensiques de Montpellier (EDPFM), Univ Montpellier, D´epartement de m´edecine l´egale, P^ole Urgences, Centre Hospitalo-Universitaire de Montpellier, 371 Avenue du Doyen Gaston Giraud, Montpellier, France*

* Corresponding author. LIRMM, Montpellier, France.
** Corresponding author. IRIM, Montpellier, France.
E-mail addresses: ganesh.gowrishankar@lirmm.fr (G. Ganesh), raphael.gaudin@irim.cnrs.fr (R. Gaudin)

Abstract

Hybrid-AI systems that integrate biological neurons require neural models to learn and remember while interacting with artificial agents. Such systems are challenging to establish given the low maturity of neuronal circuits generated *in vitro.* Here, we introduce an original hybrid-AI platform that connects an organotypic culture of *post-mortem* adult brain explant (OPAB) to a piano-playing robot composed of an anthropomorphic hand and a microphone (ear). OPABs in this platform were able to learn sensory-motor associations between piano key presses by the robot, and the sounds generated (training), and then imitate the piano notes played by humans by controlling the robot (test). This acquired bi-directional plasticity, that remained for several days, was however disrupted by pharmacological inhibition of electrical neurotransmission or upon neurotropic virus infection. Beyond possibilities for hybrid-AI systems, our work exhibit OPABs as an in-vitro learning model of the human brain that can be significant for neurosciences and virology.

Introduction

The rise of artificial neural networks, and the consequent Artificial Intelligence (AI) systems is changing our society. The ability and applications of AI have especially taken off in the last few years with the advances achieved with deep neural networks and large language models (Rumelhart et al. 1986, Krizhevsky et al., 2012; LeCun et al., 2015; Radford et al., 2018). However, these developments have also highlighted again the ecological concerns, in terms of heating and energy consumption, posed by the AI systems (Patterson et al., 2021; Masanet et al., 2020). The excitement generated by new learning structures that reduce this energy requirement and cost (Schwartz et al. 2020; Schumacher et al. 2023; DeepSeek-AI, Guo et al. 2025) shows the importance of this issue to the AI industry and the world.

Animal brains on the other hand show remarkable complexity in cellular makeup and function, that enables unique sensory-motor learning abilities, while being extremely energy efficient. For example, a zebrafish can hunt prey, avoid predators and survive (Orger et al. 2017) using only 0.2 microwatts (Webb 1971), and a human adult brain consumes 20 watts (Raichle et al. 2002). In contrast, the world's most powerful super-computers consume tens of megawatts (Konstantin et al. 2025). Animal, and especially human, brains are also very efficient in learning compared to AI systems. AlphaGo, the AI program that beat the human world champion in the Japanese game 'Go', had to be trained on over 150 000 games.

This is equivalent to over 100 years of practice by a human playing the game for 8 hours a day, which is obviously much more than what the human expert practiced. To converse like an intelligent human, ChatGPT 3 was trained on 45 TB, which is equivalent to a human reading 5 ebooks a day for 250 years (Brown et al. 2023).

Due to these characteristics, hybrid AI systems, that integrate live neurons in the processing, is seen as a promising, though still challenging, future for AI systems (Smirnova et al. 2023). Recent studies have shown the first developments for the use of *in vitro* 2D neurons (Kagan et al. 2023) and brain organoids (Cai et al. 2023) as brain models that can replace artificial neural networks. However, the two models have their disadvantages. Plasticity induction in 2D neural populations is notoriously difficult and unstable (Balci et al. 2023) and brain organoids are known to be highly heterogeneous and require delicate maintenance (Hartung et al. 2023). With this paper, we introduce *ex vivo* organotypic culture of *post-mortem* adult brain explants (OPABs) as an alternate candidate learning unit that can overcome some disadvantages. In our recent study, we have shown that OPABs can exhibit robust regional connectivity changes (Iwasaki, Bernou et al. 2024). In this study, we re-analyzed this data and added more experiments to first show that OPABs can show bi-directional plasticity, similar to previous observations of *symmetric STDP* (Mishra et al. 2016), that can last over weeks. We then exhibit the OPAB's capability to perform unsupervised learning when connected to a piano-playing robot system consisting of an anthropomorphic hand and a microphone (ear). The OPABs were able to learn sensory-motor associations between piano key presses by the robot, and the sounds these presses generate. Following this, they were able to imitate piano notes played by humans, for up to two weeks after learning.

Results

The protocol for the use of *post mortem* brain explants for research purposes included in this study was approved by the institutional review board (IRB) of the CHU (University Central Hospital) of Montpellier (approval ID: 202,000,643) and the French Biomedicine Agency (agreement number PSF20-025). It permits human brain resection for research purposes during autopsy performed at the forensics institute of the CHU de Montpellier, upon obtaining local prosecutor authorization and family non-opposition.

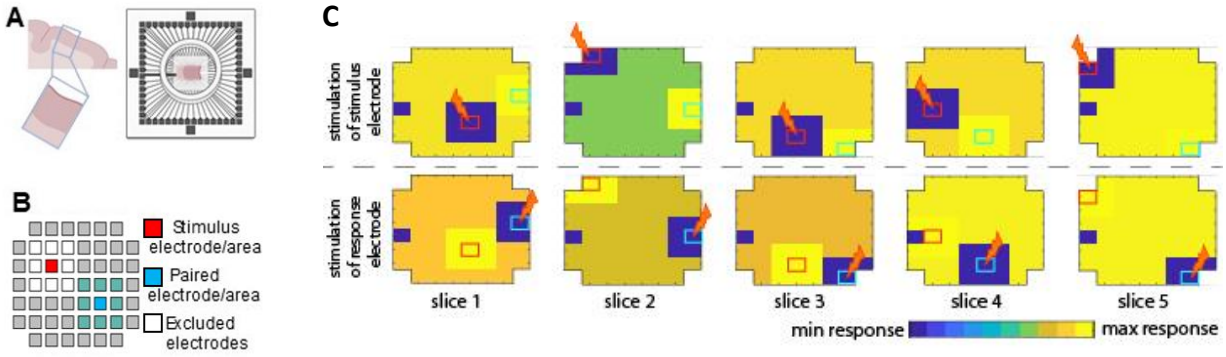

Fig 1: OPABs show bi-directional plasticity. A) The OPAB consists of a slice of the cortex of 3 mm width and 300 μm thickness placed on a microelectrode array. **B**) We selected one of the active electrode as a stimulus electrode (red) and one as the paired electrode (blue). For three days, the stimulus and paired electrodes were stimulated sequentially (12 ms interval) with 300 stimulation pairs per day for 3 days, as previously described (Iwasaki, Bernou et al. 2024). **C**) Following this procedure, we stimulated either the stimulus or paired electrode alone and observed the response across the microelectrode array. This is shown in the panels as a colourmap. The stimulation of the stimulus (red) electrode resulted in highest

response in the paired 'region' (neighborhood of the electrode). Note the higher response around the green electrode in top row of C. Importantly, the stimulation of the paired (blue) electrode of the same slice also led to highest response of the stimulus regions around it (note higher activations around the red electrode in bottom row of C) showing a bi-directional plasticity increase. Of note, the activation in the region around the stimulated electrode was removed for clarity. The electrode with a low activation in the middle left side of each panel is the ground electrode.

OPABs show symmetric spike dependent plasticity

The preparation of OPABs followed procedures as in previous studies (Iwasaki, Bernou et al. 2024) and is described in detail in the methods section. Briefly, the motor cortex from the frontal lobe of patients with short post-mortem interval (see patients' details in Table S1) was dissected and small cubes (about 0.5–1 cm^3) were cut perpendicularly to the longitudinal axis of the gyrus. The cubes were transported from the hospital to the lab within 30 min, and then sliced into 300-µm-thick sections using a vibratome. All the samples displayed cortical layers and a piece of the white matter. The slices were cultured in 6-well transwells for *ex vivo* culture at the air–liquid interface.

The OPABs were mounted on a 3D microelectrode arrays (3D-MEA (Heuschkel et al, 2002) with conical microelectrodes that penetrate up to 80 µm into the slice (Fig. 1A). Previously, we have used this setup to train regions on the OPABs with a spike-timing dependent plasticity (STDP) like protocol (Iwasaki, Bernou et al. 2024). In this protocol, we stimulated two non-neighbouring electrodes ('stimulated' electrode, followed by a 'paired' electrode) on the OPAB separated by a time gap of 12 ms. This induces an increase of connectivity, between the 'stimulated region' (the stimulated electrode and its neighborhood) and the 'paired region' (the paired electrode and its neighborhood), as quantified by the change in magnitude of response measured in the paired electrode region after training, compared to the same value before training (Iwasaki, Bernou et al. 2024). Here, in this study, we observed this increase in connectivity again in a new set of OPABs from different donors (Fig. 1C, top row). In addition to this confirmatory result, we report here that the same training, by the stimulation of the stimulus electrode followed by the paired electrode, also induces an increase of the reverse connectivity between the electrodes such that, a stimulation of the paired electrode, shows increased response in the electrodes of the stimulated region (Fig 1C, lower row). This *bi-directional* plasticity is similar to reports of symmetric plasticity in literature (Mishra et al. 2016) and is particularly interesting with regards to our goal to develop AI systems with biological components. Indeed, symmetric plasticity promises to enable immediate inversion of learnt associations. Inversion of learnt associations is not trivial for AI systems, with specific learning techniques suggested in order to achieve this (Song et al. 2024). In fact, the mechanism by which the human brain can invert learnt associations is a key question in developmental neuroscience (Jones et al. 2009) and the possible explanation provided by mirror neurons in this regard was one of the reason for their popularity when they were initially discovered (Iacoboni 2009).

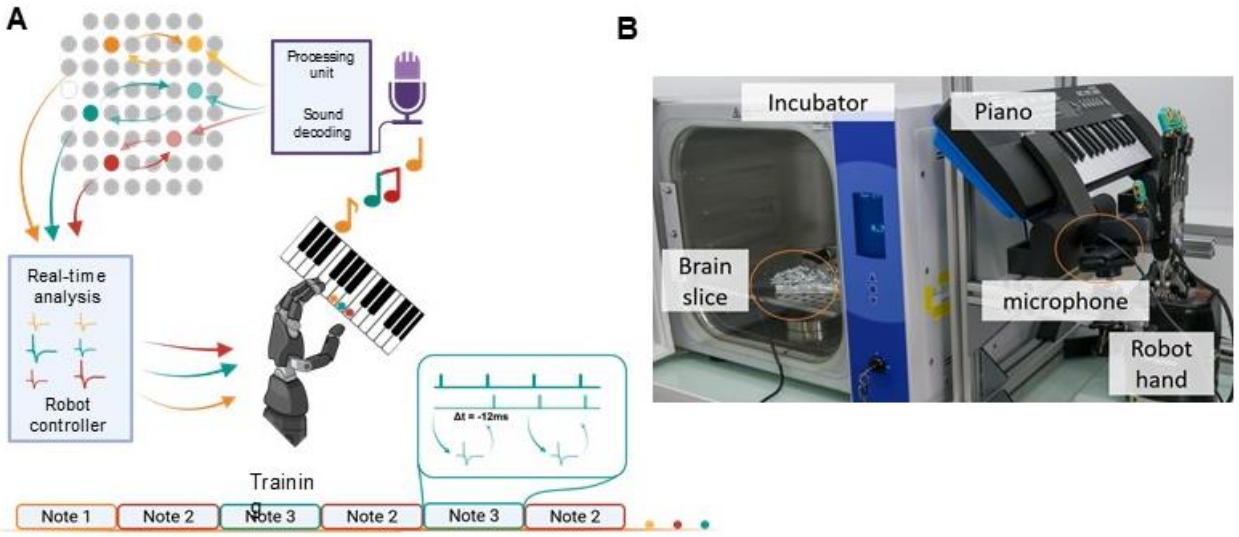

Fig 2: OPAB-Robot system and training. A) Our setup connects an OPAB in an atmosphere-controlled incubator with an anthropomorphic robot hand, and a microphone. We selected three random electrodes as 'motor electrodes', and connected it to the index, middle, and ring finger of the robot hand through a robot controller. The activation of the three motor electrodes resulted in the flexing of the associated robot finger, pressing the keys of the piano placed under the robot hand. A microphone fixed on the piano received the notes which were decoded by a sound decoder program. The decoded 'LA', 'TI', and 'DO' notes were connected back to the OPAB, so as to activate one of three 'sensory electrodes' that were also randomly selected on the OPAB. **B**) A photo of the real setup. **C**) During 'training', one of the motor electrode was activated in a block-random fashion. The notes heard by the microphone activated the corresponding sensory electrode, which was timed to coincide with the following motor electrode activation. See methods for details and video here[1] for training procedure.

Action imitation is a key skill that is believed to be enabled by the inversion of sensory-motor associations, where an agent that has learnt a mapping between his actions and resulting sensory feedbacks, is then able to generate actions (imitate) corresponding to provided sensory observations of the action. Action imitation is an important skill that enables human babies to develop new actions and skills (Jones et al. 2009) and consequently, the so called 'learning by demonstration', has been a major topic in robotics over the past decades (Hussein et al. 2017) to enable robots to copy and learn from humans. Due to these reasons, here we decided to use action imitation as a task to validate and exhibit the promising possibilities of symmetric plasticity exhibited by OPABs.

Experimental setup: A brain slice with a robot body

The human limbs are wired to specific motor neural populations in the brain cortex. As babies, we use arbitrary motor activations, referred to as 'motor babbling' in engineering communities (Caligiore et al. 2008), to observe the sensory consequences received by the neural populations in the various sensory processing areas of the cortex. Babies use motor babbling to develop motor-sensory associations and understand their body (Corbetta et al. 2009). Here we aimed to mimic this process in an hybrid-AI platform, that connects an OPAB to a robot. Our platform consists of an OPAB, mounted on a MEA, and connected to a anthropomorphic robot hand and mic to respectively serve as the hand and ear of the brain slice (Fig. 2A). A digital piano is placed near the robot, enabling the robot to press the keys by bending its fingers.

[1] https://drive.google.com/file/d/1PEsU_00nW0kjfhj4TmJkaX4svCFmK_fp/view?usp=sharing

We worked with three fingers (index, ring and middle) of the robot, that press the 'LA', 'TI', and 'DO' keys on the digital piano when they bend, respectively. We connected the three fingers to three randomly selected 'motor electrodes' on the OPAB, such that the OPAB can move these fingers (and press the piano keys) when the motor electrode is activated. The sounds heard by the mic (ears) are transmitted back to OPAB through the 'sensory electrodes'. We choose three random sensory electrodes that receive a stimulation when the mic hears a 'LA', 'TI' or 'DO' sound respectively. Two additional modules, a robot controller and a sound decoder, served as lower level processing units in the setup (see rectangles in Fig. 2A). The 'robot controller' chose the peak activation among the motor electrodes as the command from the OPAB and translated it to the finger phalange motors, in order to move a finger. A 'sound decoder' received the mic output to decode the sound notes ('LA', 'TI', and 'DO') and stimulate the corresponding sensory paired electrode. Overall, the combination of AI decoders and biological neurons makes this setup a hybrid brain-AI system that we trained to imitate a human playing notes on the piano.

Training the OPAB-Robot piano player

We worked with a total of 30 OPABs collected from 3 donors. The OPABs was primed for one day (DAY 0), using a protocol similar to Fig. 2C but where all the motor electrodes were stimulated together as 'stimulus' electrodes, followed by simultaneous stimulation of the three sensory electrodes as the 'paired' electrodes. This day served as a priming day and was used to verify that the randomly chosen motor and sensory electrodes were active and not lying over regions without neural activity. The next three days, DAY 1 to DAY 3, followed a training protocol shown in Fig. 2C where the motor electrodes were stimulated in a blocked pseudo random pattern to simulate motor babbling. Each of these stimulations led to the flexion of the robot finger, which then played the piano note. The note heard by the mic was then sent back as a stimulation to a corresponding stimulus electrode (please See Video here[2]). A total of 300 stimulations were used each day to train an OPAB.

We postulated that the training protocol would slowly lead to sensory motor associative learning enabling the OPAB to associate each finger with a corresponding sound output. Note that while we have previously shown this plasticity between a single pair of stimulus-paired electrode (Iwasaki, Bernou et al., 2024), the current protocol requires the OPAB to develop multiple independent and parallel associations. Moreover, given that the induced plasticity is bi-directional, here we expected the training to enable action imitation by the OPABs. That is, 'hearing' (as sensory electrode stimulations) a piano note will automatically activate the appropriate motor electrode to move the robot finger, and imitate the piano note. We however found that after training, while the stimulation of a stimulus electrode lead to high absolute response in the region around the motor electrode (See Fig. 1B), the peak response was sometimes in a neighbor of the motor electrode and not the motor electrode itself. This is not strange given that an electrode captures activity from a population of neurons and it is possible that the reverse connectivity increase is captured better in a neighboring electrode. Here to optimize the robot performance, we therefore started DAY 4 by utilizing the first three notes in a one-shot learning procedure (Li et al. 2006) to calibrate and connect the robot to this *peak motor electrode,* before moving on to the test sessions.

[2] https://drive.google.com/file/d/1PEsU_00nW0kjfhj4TmJkaX4svCFmK_fp/view?usp=sharing

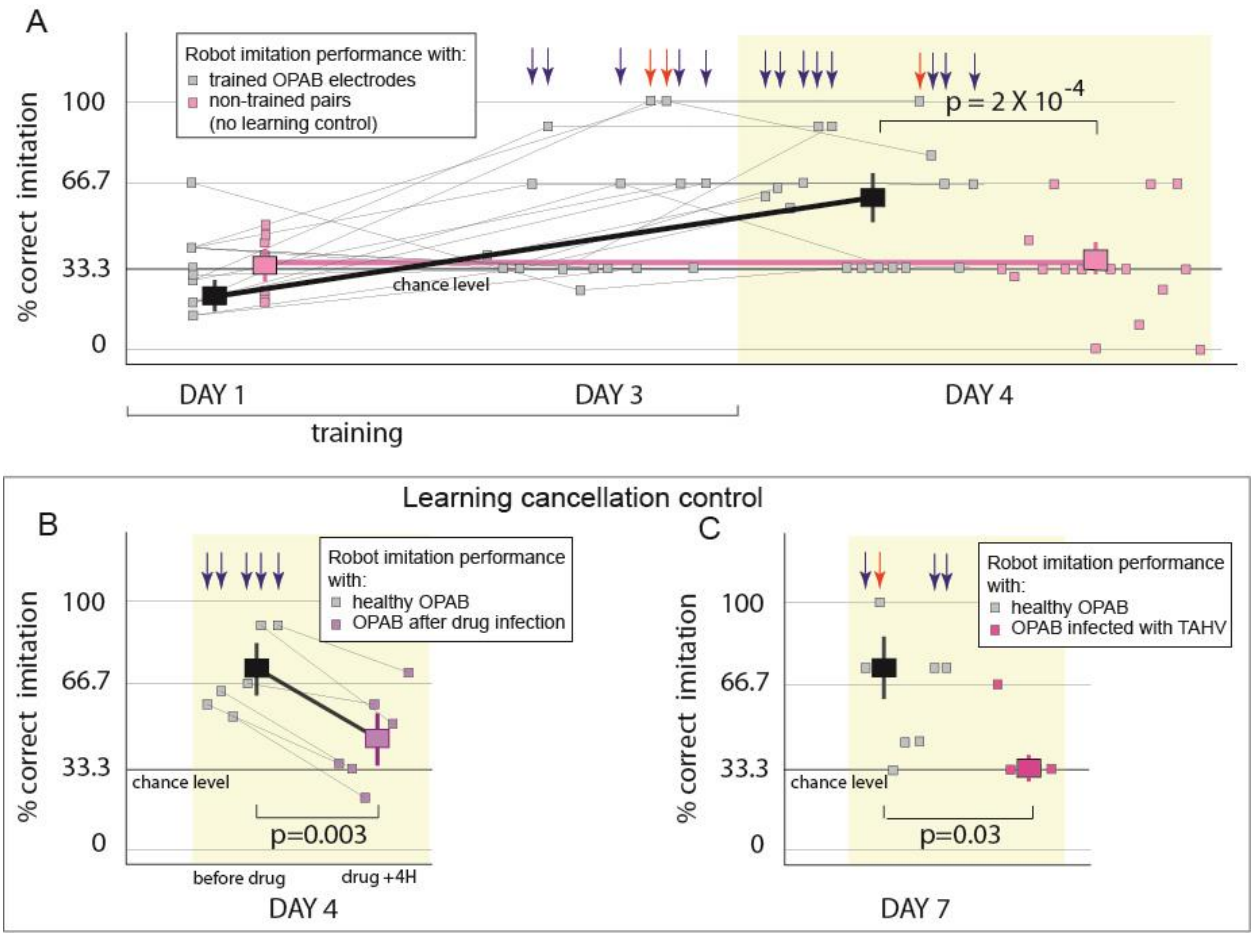

Fig 3. Robot imitation performance and controls: A) Plot of the robot imitation performance by 16 OPABs at start of training (DAY 1), last day of training (DAY 3) and during test on DAY 4. Each grey box shows the average performance during the imitation of the three notes by the robot, when connected to an OPAB (grey boxes). The larger black box shows the across OPAB average +/- SE in a day. The non-trained electrode pair (no-learning control) from the same OPABs are represented by pink squares. The red arrows on top highlight OPABs that exhibited 100% imitation performance with all the three notes, every time they were played. The blue arrows highlight OPABs that exhibited 100% imitation performance with two of the notes, every time they were played. **B**) As the first 'learning cancellation control', we compared the robot imitation performance of 6 OPABs before (grey boxes) and 4 h after (small purple boxes) the addition of 50 µM CNQX and 100 µM AP-V. The larger boxes show the average +/- SE prior (black) and after (purple) drug addition performance across the 6 OPABs. **C**) To evaluate the impact of a more physiological perturbation, we analyzed the robot imitation performance on DAY 7 after four OPAB was infected with the neurotropic Tahyna virus (TAHV) on DAY 4 (pink data points). This performance was compared with the robot imitation performance with 7 healthy OPABs on DAY 7 (grey and black data points).

<u>OPAB-Robot system imitates what it hears</u>

Following the training, we performed test sessions on DAY 4 and DAY 7 for 16 OPABs, where a human experimenter pressed piano keys in random sequences, and the robot played back the notes automatically based on associations learnt during the training phase (DAY1-3). During the test, a delay

was introduced in the sound decoder output to ensure that decoded stimulations were sent to the robot only after the human finished playing, thereby preventing simultaneous note production by both the human and the robot. Each day a human experimenter played at least 2 sets of notes, each consisting of at least 5 notes. We quantified the performance of each OPAB by analyzing the imitation accuracy of the robot over all the played notes.

The grey and black datapoints in Fig. 3A plots the overall imitation accuracy across the three notes; imitation attempts were quantified by scoring successes (1) or failures (0), with random outcome expected at 33% success (Fig. 3A). The overall accuracy is shown for each individual OPAB on the first day of training (DAY 1), the last day of training (DAY 3), and on DAY 4, following the completion (3 days) of training. The OPABs exhibited chance level performance on DAY 1 with an across OPAB accuracy of 31.22±11.7 STD% (Fig. 3A). By the end of training on DAY 4 however, three out of 16 (~19%) trained OPABs exhibited 100% imitation accuracy of all notes (OPABs indicated by red arrows). These OPABs were able to imitate all the three notes correctly, every time it was played in the test session. Furthermore, 7 (37.5%) of the OPABs exhibited 100% accuracy with two notes. These OPABs were able to imitate two of the notes correctly, every time it was played in the test session. The third note was mistaken as one of the other notes. Overall, 62.5% of the OPABs could correctly learn to imitate at least 2 notes after training, while the overall accuracy across the OPABs was seen as 58.5±23 STD % across the trained OPABS on DAY 4.

We performed three control experiments to validate the significance of the learning by the OPAB-robot system. First, as a 'no-learning control' performed on each of the 16 OPAB, we compared the imitation performance of the robot when it was connected to randomly selected untrained motor electrodes on the same OPAB (Fig. 3A, pink dataset). The performance measured with these random connections on DAY 1 was also random with an average across OPAB performance of 33.8±8.9 STD%. Crucially, the imitation accuracy of the robot when connected to the untrained motor electrodes remained low on DAY 4, with an average across OPAB performance of 36.6±18 STD%. Overall, a 2-way repeated measures ANOVA, with *association* (trained and no-learning) and *days* (DAY 1 and DAY 4) as factors, exhibited a significant interaction ($F(1,14)=93.91$, $p<0.0001$) between the factors. Post hoc t-tests indicated no difference between the performance on DAY 1 ($T(14)=2.02$, $p=0.06$) between the trained motor electrodes the non-trained controls, but a significant difference in performance was observed on DAY 4 ($T(14)=8.37$, $p < 10^{-6}$) between the robot performance when connected to the trained motor electrodes compared to when it was connected to the non-trained controls.

Second, as a 'learning-cancellation control', we treated six trained OPABs with CNQX and APV, two drugs inhibiting electrical synaptic transmission and analyzed the imitation performance before (black and grey data in Fig. 3B) and 4 h after drug treatment (pink data, Fig.3B). Upon treatment with these drugs, we observed a significant decrease of imitation performance ($T(5)=5.28$, $p=0.0032$, paired T-Test) by the robot.

Finally, as a more physiopathological control, we infected four OPABs, which exhibited more than 66.7% correct imitation performance, with the neurotropic Tahyna virus (TAHV) on DAY 4 and evaluated the imitation performance on DAY 7. We previously showed that exposure to TAHV significantly perturbed electrical activity of OPABs (Partiot, Gorda et al, EMBO Mol Med, 2024), and hence, we hypothesized that this could lead to an attenuation of the association learning developed during the training. Fig. 3C compares the performance of the robot with the infected OPABs on DAY 7 (Fig. 3C, pink data) with a robot connected to non-infected OPABs (seven in total) on DAY 7 (Fig. 3B, grey and black data). The healthy OPABs exhibited a significantly higher imitation performance compared to the OPABs that suffered the virus infection ($Z(10)=54$, $p=0.03$, Wilcoxon Ranksum test).

Discussion

This work presents two key results. First, we show that *post-mortem* adult brain explants (OPABs) can exhibit robust bi-directional plasticity between multiple region pairs. Second, we show that this can be used to induce sensory-motor associative learning and enable imitation learning by a robot. In our study, 62.5% of OPABs could learn at least 2 notes out of three, showing that OPABs can learn. These results are in fact pessimistic, due to the way we chose the stimulation and paired electrodes, and can be improved further, as discussed below. We also observed that the induced plasticity is robust and can be maintained for many days. While in Fig. 3 we show that the OPABs retain associative learning for up to 7 days after the end of training, we have also conducted longitudinal studies with 5 OPABs, four of which retained learning for at least 17 days after training. Two of these OPABs exhibited 100% imitation performance with every note after 17 days, while two OPABs exhibited 100% performance with 2 notes giving 66.7 % overall performance, and the fifth OPAB could not learn. These results highlight *post-mortem* brain slices as a promising brain model to serve in hybrid-AI systems, that integrate live neurons in the processing.

In our current study, we show the ability of OPABs to learn three parallel motor-sensory associations through a hybrid neurobiorobotic system. The choice of *three* associations was limited by the size of the OPABs, which was around 5 mm in diameter, and the resolution of our microelectrode array, which limited the spatial localization of the stimulations we could achieved. We believe that higher numbers of parallel connections may be possible with larger brain slices, higher resolution of electrodes, and/or both. Even with three pairs, we observed that parallel training induced localization issues leading to interference between learnt associations. Consequently we observed that unlike our previous work (Iwasaki, Bernou et al. 2024), where we averaged the activity in the region around the stimulated electrode, utilizing the peak electrode to determine an associated electrode was more robust across trials in this study. On the other hand, it is important to note that we chose the three motor electrodes and three sensory electrodes randomly (just ensuring that they are not neighbors, see methods for details). This procedure was followed for two reasons. Primarily, we wanted to illustrate that OPABs can make three parallel associations between *any* pair of motor and sensory electrodes, and to emphasize that the learning was not optimized to utilize innate connectivities within an OPAB. Furthermore, this procedure better simulates the sensory-motor associations learnt in an infant brain, that are made between arbitrary actions and their sensory consequences (Corbetta et al. 2009). We did use a priming session to make sure that we do not choose electrodes over inactive neurons, but the random choices may still mean that in some cases the chosen electrodes may have been over neuron populations that were damaged or not innately connected to each other, which is crucial to exhibit plasticity. The inability to reproduce notes by some of our OPABs in the study may therefore be because of an 'unfortunate' selection of electrodes. The learning results can therefore be arguably improved in future studies with an activity-oriented selection to choose the motor and sensory electrodes.

Our understanding of sensorimotor functions suffers from a gap of knowledge when changing scale between behavioral level learning and neuronal learning *in vitro*. Rodent models are instrumental in our understanding of neurocognition, but there are extensive differences between homologous human and mouse cell types (Hodge et al, 2019). In human context, associative learning (which the authors called "sentience") was shown in cultured neurons (Kagan et al, 2022), and we also previously reported that long term potentiation can be induced in OPABs (Iwasaki, Bernou et al, 2024). Yet, these studies cannot fully embrace the complexity of sensorimotor learning as there were no interactions with a physical environment. Neurobiorobotics is at the forefront of bionic prostheses development that attain more human-like function with effective sensorimotor restoration (Paul et al, 2021), but in sharp contrast, the embodiment of biological neural systems *in-a-dish* remains mostly unexplored (see review by Bartolozzi

et al, Nature Com, 2022). The concept of 'organoid intelligence' has been pushed forward in recent years (Smirnova et al, 2023), showing promising capabilities for basic learning and memory (Alam et al, 2025) and the development of hybrid-AI systems (Cai et al, 2023; Smirnova et al, 2024). Although organoids do not exhibit the cellular diversity and synaptic maturity of adult brain explants, the tremendous efforts made to develop pipelines to induce robust synaptic reinforcement in organoids (Khajehnejad et al, 2025; Osaki et al, 2024) will make this model a relevant alternative to perform associative learning *in vitro* in the near future. So far, the use of OPAB likely represents the closest *in-a-dish* surrogate to the human brain, and our setup provides the first platform where a robot can exchange information with a neural model in a closed-loop system for the study of human sensorimotor learning *in vitro*. Furthermore, we confirmed that no hardware/software artifact was responsible for the observed learning, by showing that the inhibition of AMPA and NMDA receptors (using CNQX and APV antagonists respectively) prevented learning, a finding consistent with the established role of glutamate receptors in learning (Hasan et al, 2013; Hoy et al, 2012).

To apply our hybrid system to a more physiopathological context, we investigated how a neuroinfection can impact learning. Numerous viruses have been associated with cognitive impairments (Bouget et al, Trends Neurosci, 2025), and we recently showed that TAHV, a neurotropic virus associated with CNS disease (Edridge et al, 2020), perturbs electrical activity of OPAB (Partiot, Gorda et al, EMBO Mol Med, 2024). Of note, despite its high prevalence, TAHV is usually asymptomatic in humans, although potential TAHV-associated neurocognitive symptoms may have passed under traditional clinical surveillance. Here, we show that TAHV infection abolishes the learned connectivity recapitulated in our hybrid platform, further illustrating the potential of our model for medical investigations. Further work will be needed to understand the molecular mechanisms associated with TAHV-induced neural dysfunctions and evaluate the neurocognitive risk posed by orthobunyaviruses, which may have been overlooked.

Our experiment tried to copy the motor-sensory associative learning exhibited by developing brains, where actions are used to observe sensory consequences and make corresponding Hebbian associations, through increased connectivity (Corbetta et al. 2009). The bi-directional nature of these connectivites (Fig. 1B) enabled us to then make actions (finger movement imitation), given the sensory consequence (auditory notes). We did use two AI units in the system, a robot controller to decide the phalange motor movements corresponding to a chosen finger, and a sound decoder to decode the notes from the microphone signals. However, note that the finger choice itself is performed by the brain slice automatically (utilizing its associative training). We note that we do not provide any error feedback to the OPAB during the learning, and what we exhibit here is the ability of OPABs to perform unsupervised motor-sensory associative learning. While this is arguably the most basic learning mechanism in our brain, here we show that it is possible in *ex vivo* human brain explants, and provide a procedure to enable robust associations that last over weeks. Multiplication of the number of parallel associations and addition of an error-feedback related learning component to the basic learning mechanism, can enable future studies to slowly replicate the learning abilities of the human brain in vitro. Together, our work presents a new approach to model associative learning *in-a-dish,* that can be a tool to study cognitive virology and neuroscience, and can provide conceptual and technical insights that will contribute to the future of human neuro-robotics and hybrid-AI systems.

Acknowledgement

The following reagent was obtained through BEI Resources, NIAID, NIH: Tahyna Virus, 92, NR-541. Funding: Human Frontiers Science Program (HFSP) grant (RGP012/2024-101) to RG and GG. Agence Nationale de la Recherche (ANR) CIBORG (ANR-21-CE33-0007-03) to SC, RG and GG, and isiBrain (ANR-

22-CE15-0007-01) to RG and SC; and ANR-MRSEI2023 MAVERIC to GG and RG. This project has received financial support from the CNRS through the MITI interdisciplinary programs. The authors acknowledge Jules Bouget for his help in the preparation of the brain slices and Alicia Trausch for recording and editing the experiment videos.

References

Alam El Din, D. M., Moenkemoeller, L., et al. (2025). Human neural organoid microphysiological systems show the building blocks necessary for basic learning and memory. Communications Biology, 8, 1237. https://doi.org/10.1038/s42003-025-08632-5

Backus, J. (1978). Can programming be liberated from the von Neumann style? A functional style and its algebra of programs. Communications of the ACM, 21(8), 613–641. https://doi.org/10.1145/359576.359579

Balci, F., Ben Hamed, S., et al. (2023). A response to claims of emergent intelligence and sentience in a dish. Neuron, 111(5), 604–605. https://doi.org/10.1016/j.neuron.2023.02.009

Bartolozzi, C., et al. (2022). DishBrain plays Pong and learns via dopamine-like reward signal. Nature Communications, 13, 2511. https://doi.org/10.1038/s41467-022-28487-2

Bouget, J., et al. (2025). When viral infections rewire neural circuits: Towards cognitive virology. Trends in Neurosciences, 48(12), 964–976.

Brown, A., Jones, T., Garcia, L., & Williams, K. (2023). Enhancing context understanding in ChatGPT: Advancements and challenges. Proceedings of the International Conference on Natural Language Processing.

Cai, H., Ao, Z., et al. (2023). Brain organoid computing for artificial intelligence. bioRxiv. https://doi.org/10.1101/2023.02.28.530502

Caligiore, D., Ferrauto, T., et al. (2008). Using motor babbling and Hebb rules for modeling the development of reaching with obstacles and grasping. CogSys 2008: International Conference on Cognitive Systems. Karlsruhe, Germany.

Corbetta, D., & Snapp-Childs, W. (2009). Seeing and touching: The role of sensory-motor experience on the development of infant reaching. Infant Behavior and Development, 32(1), 44–58. https://doi.org/10.1016/j.infbeh.2008.10.004

DeepSeek-AI, Guo, D., et al. (2025). DeepSeek-R1: Incentivizing reasoning capability in LLMs via reinforcement learning. arXiv. https://arxiv.org/abs/2501.12948

Edridge, A. W. D., & van der Hoek, L. (2020). Emerging orthobunyaviruses associated with CNS disease. PLOS Neglected Tropical Diseases, 14(10), e0008856. https://doi.org/10.1371/journal.pntd.0008856

Hartung, T., Morales Pantoja, I. E., & Smirnova, L. (2024). Brain organoids and organoid intelligence from ethical, legal, and social points of view. Frontiers in Artificial Intelligence, 6, 1307613. https://doi.org/10.3389/frai.2023.1307613

Hasan, M., Hernández-González, S., et al. (2013). Role of motor cortex NMDA receptors in learning-dependent synaptic plasticity of behaving mice. Nature Communications, 4, 2258. https://doi.org/10.1038/ncomms3258

Heuschkel, M. O., Fejtl, M., et al. (2002). A three-dimensional multi-electrode array for multi-site stimulation and recording in acute brain slices. Journal of Neuroscience Methods, 114(2), 135–148. https://doi.org/10.1016/S0165-0270(01)00514-3

Hodge, R. D., Bakken, T. E., et al. (2019). Conserved cell types with divergent features in human versus mouse cortex. Nature, 573(7772), 61–68. https://doi.org/10.1038/s41586-019-1506-7

Hoy, K. C., Huie, J. R., & Grau, J. W. (2013). AMPA receptor mediated behavioral plasticity in the isolated rat spinal cord. Behavioral Brain Research, 236(1), 319–326. https://doi.org/10.1016/j.bbr.2012.09.007

Hussein, A., Gaber, M. M., et al. (2018). Imitation learning: A survey of learning methods. ACM Computing Surveys, 50(2), Article 21. https://doi.org/10.1145/3054912

Iacoboni, M. (2009). Imitation, empathy, and mirror neurons. Annual Review of Psychology, 60, 653–670. https://doi.org/10.1146/annurev.psych.60.110707.163604

Iwasaki, Y., Bernou, C., et al. (2024). Organotypic culture of post-mortem adult human brain explants exhibits synaptic plasticity. Brain Stimulation, 17(5), 1018–1023. https://doi.org/10.1016/j.brs.2024.08.010

Jones, S. S. (2009). The development of imitation in infancy. Philosophical Transactions of the Royal Society B: Biological Sciences, 364(1528), 2325–2335. https://doi.org/10.1098/rstb.2009.0045

Kagan, B. J., Kitchen, A. C., et al. (2022). In vitro neurons learn and exhibit sentience when embodied in a simulated game-world. Neuron, 110(23), 3952–3969.e8. https://doi.org/10.1016/j.neuron.2022.09.001

Khajehnejad, M., Habibollahi, F., et al. (2025). Dynamic network plasticity and sample efficiency in biological neural cultures: A comparative study with deep reinforcement learning. Cyborg and Bionic Systems, 6, 0336. https://doi.org/10.34133/cbsystems.0336

Konstantin, F. P., Sanders, J., et al. (2025). Trends in AI supercomputers. arXiv. https://arxiv.org/abs/2504.16026

Krizhevsky, A., Sutskever, I., & Hinton, G. E. (2012). ImageNet classification with deep convolutional neural networks. Advances in Neural Information Processing Systems, 25, 1097–1105.

LeCun, Y., Bengio, Y., & Hinton, G. E. (2015). Deep learning. Nature, 521(7553), 436–444. https://doi.org/10.1038/nature14539

Li FF., Fergus R. & Perona P. (2006). One-shot learning of object categories, in *IEEE Transactions on Pattern Analysis and Machine Intelligence*, vol. 28, no. 4, pp. 594-611. doi: 10.1109/TPAMI.2006.79.

Marasco, P. D., et al. (2021). Neurorobotic fusion of prosthetic touch, kinesthesia, and movement in bionic upper limbs promotes intrinsic brain behaviors. Science Robotics, 6(56), eabf3368. https://doi.org/10.1126/scirobotics.abf3368

Masanet, E., et al. (2020). Recalibrating global data center energy-use estimates. Science, 367(6481), 984–986. https://doi.org/10.1126/science.aba3758

Mishra, R. K., Kim, S., Guzmán, S. J., & Jonas, P. (2016). Symmetric spike timing-dependent plasticity at CA3–CA3 synapses in the hippocampus. Nature Communications, 7, 11552. https://doi.org/10.1038/ncomms11552

Orger, M. B., & de Polavieja, G. G. (2017). Zebrafish behavior: Opportunities and challenges. Annual Review of Neuroscience, 40, 125–147. https://doi.org/10.1146/annurev-neuro-071714-033857

Osaki, T., Duenki, T., et al. (2024). Complex activity and short-term plasticity of human cerebral organoids reciprocally connected with axons. Nature Communications, 15, 2945. https://doi.org/10.1038/s41467-024-46787-7

Partiot, E., Gorda, B., et al. (2024). Organotypic culture of human brain explants as a preclinical model for AI-driven antiviral studies. EMBO Molecular Medicine, 16(5), 1004–1026. https://doi.org/10.1038/s44321-024-00039-9

Patterson, D., et al. (2021). Carbon emissions and large neural network training. arXiv. https://arxiv.org/abs/2104.10350

Pilz, K. F., Sanders, J., Rahman, R., & Heim, L. (2025). Trends in AI supercomputers. arXiv. https://arxiv.org/abs/2504.16026

Radford, A., et al. (2018). Improving language understanding by generative pre-training (OpenAI Technical Report). OpenAI. https://cdn.openai.com/research-covers/language-unsupervised/language_understanding_paper.pdf

Raichle, M. E., & Snyder, A. Z. (2007). A default mode of brain function: A brief history of an evolving idea. NeuroImage, 37(4), 1083–1090. https://doi.org/10.1016/j.neuroimage.2007.02.041

Rojas, R., & Hashagen, U. (Eds.). (2000). The first computers: History and architectures. MIT Press.

Rumelhart, D., Hinton, G., Williams, R. (1986) Learning representations by back-propagating errors. Nature 323, 533–536. https://doi.org/10.1038/323533a0

Schumacher, K., et al. (2023). Towards energy-efficient deep learning. arXiv. https://arxiv.org/abs/2303.01980

Schwartz, R., et al. (2020). Green AI. Communications of the ACM, 63(12), 54–63. https://doi.org/10.1145/3381831

Smirnova, L., Caffo, B. S., et al. (2023). Organoid intelligence (OI): The new frontier in biocomputing and intelligence-in-a-dish. Frontiers in Science, 1, 1017235. https://doi.org/10.3389/fsci.2023.1017235

Webb, P. W. (1970). Some aspects of the energetics of swimming fish with special reference to the cruising performance of rainbow trout [Doctoral dissertation, University of Bristol].

von Neumann, J. (1945). First draft of a report on the EDVAC. University of Pennsylvania. https://doi.org/10.6028/jres.141.ac (reprint)

Methods and Supplementary figures for

Ethics and donor selection

The protocol for the use of post mortem brain explants for research purposes included in this study was approved by the institutional review board (IRB) of the CHU of Montpellier (approval ID: 202000643) and the French Biomedicine Agency (agreement number PSF20-025). It permits human brain resection for research purposes during autopsy performed at the forensics institute of the CHU de Montpellier, upon obtaining local prosecutor authorization and family non-opposition. Excluding criteria were causes of death involving the head and neck (e.g. car crashes, stroke), and previously known severe neuropathology (e.g. epilepsy, neurodegenerative diseases). The data presented in this study originates from 3 donors with post-mortem interval (PMI) below 12 h (see Table S1 for details).

Slice preparation

Post-mortem human brain organotypic explants were prepared and maintained in culture as previously described (Partiot et al, 2024; Iwasaki et al., 2024). Briefly, primary motor cortex pieces were recovered at autopsy, and were sliced with a vibratome (PELCO Easyslicer, Ted Pella) into 300 µm-thick brain slices. The slices were prepared in the same way, containing white matter and the cortical layers, and maintained at the air-liquid interface on Polyethylene Terephthalate (PET) membrane inserts with 0.4 µm pores (Sabeu), hanging over 2.5 ml of medium containing Neurobasal media (Thermofisher) supplemented with N2 (Gibco), Glutamax (Thermofisher), and 0.5% Penicillin/Streptomycin (P/S, Thermofisher). Medium was changed every 2-3 days. Slices were cultured at 37°C and 5% CO_2 in 95% humidity atmosphere for at least 4 days prior experimentation. For electrophysiology, brain slices were plated on MEAs for 24 h prior to experiment in 150 µL artificial Cerebro-Spinal Fluid (aCSF) BrainPhys (StemCell Technologies), supplemented with N2 (Gibco), Glutamax (Thermofisher), and 0.5% Penicillin/Streptomycin (Thermofisher), with medium changed twice per day.

System Setup

As shown in Fig. 2, our setup consisted of an OPAB placed on a microelectrode array (MEA), and maintained in an atmosphere-controlled incubator. We utilized the MEA2100-systems from MCS (multichannel systems), connected to a computer via a USB serial cable. A customized C# program, utilizing the official SDK provided by the MEA provider, was used to monitor the neural electrical activity on the OPAB and deliver of electrical stimulation/s where and when required. An anthropomorphic robot hand (The Shadow Dexterous Hand, Shadow Robot, website), served as the body for the OPAB. The hand was operated by a 'robot controller' programmed in C++, that took a finger choice (index, middle or ring finger) as input, and generated the phalange movements to generate a flexing movement. An electronic piano was strategically placed below the robot hand, such that the flexion of the index, middle and ring fingers led to the pressing of the 'LA', TI' and 'DO' notes on the piano respectively. A microphone (BUFFALO Inc.) placed near the piano served as the 'ear' for the OPAB. The sound from the microphone was analyzed by a custom C# application, that decoded the played notes in real time as "LA," "TI," and "DO." The robot controller and sound decoder were implemented on one computer, which communicated with the MEA control computer via an Ethernet cable.

Table S1: Patient Donor details

	DONOR 1	DONOR 2	DONOR 3
Sex (Male/Female)	F	M	F
Age	69	54	35
Cause of death	cardiological	asphyxial death by hanging	sodium nitrite poisoning
Known treatment	antimetabolites,anti-hypertensives, anti-anxiety, anti coagalant, antacid medicine, pain killers	unknown	anti epilepsy, anti-anxiety
Comorbidities	drug addiction ,coronary artery disease	unknown	depression, suicide attempts
BMI	very slim	very slim	medium build
Corticosteroid treatment	N	N	N
Post-mortem delay	<5	<1	<2
Use	Fig. 3 A,B,C		Fig. 3C, longitudinal study

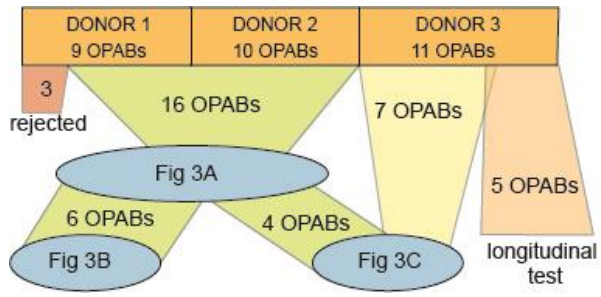

Fig. S1: OPAB utilization chart

Protocol

Our experiments extended over several days, and consisted of a *Priming* on DAY 0, followed by *Training* between DAY 1 and DAY 3. This was followed by *Tests* on DAY 4 and DAY 7. Some OPABS were tested up till DAY 17. In total, we tested 30 OPABs from 3 donors. 3 OPABs were rejected as they were not tested after infection due to technical issues. The complete structure of OPAB usage in the main and control experiments, and their presentation in the various figures is shown in Figure. S1. The donor information is provided in Table S1.

Setup and Priming

On DAY 0, after placing the brain slice on the MEA, the brain slice and MEA were installed within the incubator. Six electrodes were selected randomly from among the 60 available electrodes—three as motor electrodes (M1, M2, M3) and three as sensor electrodes (S1, S2, S3), but following the rule that any two electrode was separated by at least one electrode between them. To ensure that the selected

electrodes captured neuronal activity, the experimenter monitored the recorded electrical activity from the electrodes for approximately one minute, and re-selected any electrode on which no spike was observed within this period.

After the electrode selection, a priming protocol was used on DAY 0. Following the protocol described in Iwasaki et al. 2024, electrical stimulation with a specified waveform was applied simultaneously to M1, M2, and M3, followed 12 ms later by a simultaneous stimulation of S1, S2, and S3. This paired stimulation was delivered at a frequency of 1 Hz for 5 minutes, followed by a 1-minute stimulation-free interval. This cycle was repeated four times. Crucially, note that the simultaneous stimulation of all the motor followed by all the sensory electrodes meant that the DAY 0 stimulations did not aid in the development of specific associations. However, our preliminary studies exhibited that the priming aids the associative learning after.

OPAB Training

Following the priming, the OPAB-Robot system was allowed to train the individual (three) motor-sensory association between DAY 1 to DAY 3. A blocked random protocol, in which randomly one of the motor electrode was stimulated 5 times in each block, was used to stimulate the motor electrodes (See Fig. 2A, lower panel). Each motor electrode stimulation led to the robot finger pressing one key on the piano keyboard, aided by the robot controller. This then led to a musical note, which was heard by the microphone. The microphone signals were analyzed by the sound decoder and we stimulated electrode S1, S2 or S3 corresponding to the decoded note, 'LA', 'TI', or 'DO' respectively. Note that this whole cycle took around 500 ms, while in our protocol the stimulation of the paired electrodes needs to be after 12 ms of the stimulated electrode (Iwasaki et al. 2024). To achieve a sensory electrode stimulation after 12 ms of a motor stimulation, here we used a trick and offset the initial and paired stimulations. That is, after decoding the piano note corresponding to a motor electrode stimulation, we did not stimulate the corresponding sensory electrode immediately, but waited and did so exactly 12 ms after the next (same) motor electrode stimulation in the block (see Fig. 2A, lower panel). This protocol leads to the absence of a paired stimulation for the first motor stimulation of every block, but ensures precise timing between the motor and sensory electrode stimulations even in the presence of the processing delays. Overall, the stimulation profiles for the motor electrodes were identical to those used on DAY 0. The robot hand performed the key presses at a frequency of 1 Hz. Four 5-minute training cycles were conducted on each day between DAY 1 and DAY 3, with a 1-minute rest between each cycle. Each day, every finger underwent 100 training activations. For logistical reasons, for some of the OPABS we performed the training by simulating the robot movement and note decoding within the computer, without actually running the robot through the training period.

A response test was conducted before and after the training cycles on each day in which the stimulations were delivered individually to each of the motor electrodes, and each of the sensory electrodes ten times at 1 Hz, while the response of all electrodes was recorded for each stimulation. These were used to assess the change in forward and backward connectivity between the electrodes over the training days.

Peak electrode calibration

Following the associative training of the motor and sensory electrodes, when we stimulated the sensory electrode, we observed that while the region around the motor electrode responded heavily (See Fig. 1B), the peak response was observed sometimes in a neighbor of the motor electrode and not the motor electrode itself. Furthermore, as in our previous study (Iwasaki et al. 2024), we observed that the backward connectivity, and hence the response of the motor electrode, sometime showed an increase and sometimes a decrease over the training. We therefore started DAY 4 by calibrating this *peak motor electrode*. We stimulated each of the three sensory electrode once. Following each stimulation, we noted the peak electrode in the 3X3 neighborhood (region) of the associated motor electrode that showed highest connectivity (response) to the stimulation. This electrode was denoted as the *peak motor electrode* for the sensory electrode, and the robot finger was connected to it. We also noted the direction of response on this electrode (whether it showed an increase or decrease of response relative to DAY1). This calibration procedure corresponds to a so-called *one-shot learning* procedure (Li et al. 2006). However, importantly, note that the search for the peak electrode is localized to the immediate neighborhood of each motor electrode (and not the whole electrode matrix), and that it is done with a single (first) stimulation on a stimulus electrode. The three *peak motor electrodes* and the response direction were used for all the test validations that followed.

Robot imitation: OPAB Test

The test experiments performed DAY 4 onward aimed to evaluate if the robot can imitate what it hears. That is, whether stimulation of a sensor electrode can elicit activation in the right motor electrode so as to enable the robot to play the same note. The data processing and procedure followed to test the imitation were as follows.

A human experimenter demonstrated a series of notes (ranging from 10-18 notes) each day. The sound decoder decoded each note heard by the microphone. Following the demonstration end, the program sent five consecutive stimuli to the sensory electrode corresponding to each note played in the demonstration. Note that we avoid sending to the OPAB each note as they came in, in order to avoid that the robot starts playing the notes when the human is still demonstrating.

We averaged the activation (mean signal amplitude during the 1-second window following each of the five sensor stimulations) of each peak motor electrode. The pre-training baseline (average of the maximum responses across 10 stimulations obtained before training on DAY 1 for the same electrode) was subtracted from the activation to achieve the corresponding *motor electrode response*. Following the OPAB training, we expected the correct peak motor electrode to respond the most, and hence the *most responsive* motor electrode was chosen as the motor electrode to play the finger. Once the motor response for each demonstrated note was determined, the program sent this to the robot controller in order to move the corresponding robot finger.

As mentioned earlier, between 10 and 18 notes were played in a random order every day for testing each OPAB. The validation accuracy was calculated across all notes by determining the proportion of notes for which the brain slice exhibited a correct response. The overall accuracy was plotted for the robot when operated by each OPAB, and the overall accuracy across the OPABs, for each day in Fig. 3A.

Controls

We performed three control experiments to evaluate the training:

First, the 'no-learning' control examined the performance of each trained OPAB with an electrode pair that was not trained. For this, during the test session, while the sensory electrodes were maintained the same, three new peak motor electrodes were selected randomly and used to operate the robot. Each new *control* motor electrode was selected while avoiding a selection in the neighbourhood of the electrode it replaces, but otherwise the selection followed the rules as the original pairs (see Setup and Priming section). The simulated imitation performance of the robot was examined in this control for each OPAB, and for the same tested notes, on DAY 1 and DAY 4 and plotted in Fig. 3A in pink. The trained, and no-learning control behaviors were analyze using a 2-way repeated measures ANOVA, with the factors 'days' which had 2 levels for DAY 1 and DAY 4, and 'association', which had two levels for trained and no-learning. The control verified that even when the sensory electrodes were same, connection to any untrained motor electrode cannot enable the robot to perform the imitation. Note that all testing and performance quantification procedures were same in the no-learning control, as in the main experiment.

Second, the drug-based *learning-cancellation control* verified that a physiological attenuation of the learnt association can attenuate the robot performance and highlighted the physiological nature of the trained association. To this end, chemical inhibition of synaptic activity was performed using a combination of 50 µM CNQX and 100 µM AP-V (Sigma-Aldrich) in aCSF media. The imitation performance of the robot was tested before drug addition, and 4 h after drug addition (Fig. 3B). After checking of normality of the performance data, the performance was compared with a paired T-test to evaluate the effect of the drug addition on the association learning.

Third, we also performed an infection-based *learning-cancellation control.* For this control, four of the trained OPABs (that reached at least 66.7% performance) were infected with the Tahina virus (TAHV) as previously described (Partiot et al., 2024) on DAY 4. Upon overnight incubation, OPABs were washed 3 times and 150 µl aCSF was added. Media was changed twice a day, and robot imitation performance was measured at DAY 7 to assess for learning efficacy. This performance was compared with the imitation performance of seven (healthy) OPABs that were trained for 3 days and tested on DAY 7 without any intervention in between (Fig. 3C). The infected OPAB performance was non-normal, so we used a Wilcoxon ranksum test to compare the robot performance with the infected OPABs and the healthy OPABs.

Virus production

Vero E6 cells (CRL-1586) were obtained from the American Type Culture Collection (Virginia, WV, USA) and grown in DMEM (Sigma-Aldrich) supplemented with 10% fetal bovine serum (FBS, SigmaAldrich) and 1% P/S, Tahyna virus (TAHV, NR-541) was obtained from the American Type Culture Collection through BEI Resources. Propagation and production of TAHV stocks was performed in Vero E6 cells as previously described (Partiot, Gorda et al, EMBO Mol Med, 2024). Briefly, 80% confluent cell culture was infected with TAHV at a multiplicity of infection (MOI) of 0.0001 per cell (viral stock diluted in DMEM culture with 2% FBS, 1% P/S). The cells were incubated at 37 °C for 1 h, with gentle moving from side to side every 15

640 min. The inoculum was removed and the cells were incubated for 48–72 h at 37 °C with fresh DMEM, 2%
641 FBS, 1% P/S. Medium was spinned at 2000 × g for 10 min, supernatant harvested and titrated using plaque
642 assay titration. OPABs were infected with TAHV at DAY 4 post-training with 10^6 Plaque-Forming Units
643 (PFU).

644

Supplementary Files

This is a list of supplementary files associated with this preprint. Click to download.

- ExperimentanddataanalysisCode.zip
- Iwasakiet.alshortvideo.mp4